Shear behavior of polymer micro-scale truss structures formed from self-propagating polymer waveguides

Alan J. Jacobsen[1/2,*], William Barvosa-Carter[1], Steven Nutt[3]

1. HRL Laboratories, LLC Malibu, CA, USA
2. Department of Aerospace and Mechanical Engineering, University of Southern California, Los Angeles, CA, USA
3. Department of Chemical Engineering and Materials Science, University of Southern California, Los Angeles, CA, USA

Abstract: The shear behavior of micro-scale truss structures formed from a three-dimensional interconnected pattern of self-propagating polymer waveguides was investigated. These structures had sub-millimeter size features and comprised a repeating octahedral-type unit cell designed to suppress bending in the truss members prior to initial failure. For a typical shear loading method, the experimentally measured shear moduli deviated from predicted values as the relative density decreased. However, the mechanical behavior changed when the shear loading condition was altered to distribute the load more uniformly between all truss members and the measured shear modulus was aligned with predicted values. The shear strength and total plateau strain of these structures were strongly dependent on the mode of failure and the uniformity with which the truss member failure was distributed through the thickness of the structure. Furthermore, plateau strains of up to 60% were achieved when all truss members in compression buckled uniformly. Thermo-oxidation reaction of the polymer micro-truss structures caused an increase in the shear modulus and maximum shear strength (up to 2.9 MPa), although oxidized structures fractured at the maximum shear strain.

Key words: Mechanical properties; Cellular solids; Polymer waveguides; Lithography; Rapid prototyping

*Corresponding author:: HRL Laboratories, LLC Malibu, CA, USA. Tel.: +1 310 317 5398; fax: +1 310 317 5840. E-mail: ajjacobsen@hrl.com

Please cite this article as: Alan J. Jacobsen, William Barvosa-Carter, Steven Nutt, **Shear behavior of polymer micro-scale truss structures formed from self-propagating polymer waveguides**, Acta Materialia, Volume 56, Issue 6, April 2008, Pages 1209-1218, ISSN 1359-6454, http://dx.doi.org/10.1016/j.actamat.2007.11.018.

1. Introduction

Shear loading conditions are commonly encountered in engineering applications, and thus understanding the shear response of new materials and structures is essential. The shear behavior of cellular materials, i.e. materials with significant porosity, is governed primarily by the cellular architecture and the uniaxial properties of the solid material of which they are comprised [1]. For a cellular material with a randomly oriented architecture, Gibson and Ashby [1] have shown that the cell struts tend to exhibit bending under mechanical load. However, for ordered, truss-like cellular architectures, bending of the cell struts can be suppressed, improving the modulus and strength of the bulk cellular material [2], [3] and [4].

Investigations of the shear behavior of truss-type cellular materials that exhibit stretch-dominated deformation modes are fairly limited, partly because of the shortage of suitable synthesis methods. One technique for creating cellular materials with micrometer-scale truss features involves folding a two-dimensional grid (formed using soft lithography and subsequent electrodeposition) into a three-dimensional truss structure. Brittan et al. [5] tested a beam formed through this technique under four-point bending, which exerted a constant shear force on a portion of the truss structure. Although, the bending stiffness and strength were less than a simple box beam of equivalent weight, the truss structure afforded the opportunity for optimization, which they reported could greatly enhance the mechanical performance.

Larger-scale metallic lattice structures are another category of cellular material with an ordered truss topology. Metallic lattice structures have been formed by various methods [4] and [6] and studied under shear-loading conditions [7], [8], [9], [10], [11] and [12]. Different cellular architectures have

Please cite this article as: Alan J. Jacobsen, William Barvosa-Carter, Steven Nutt, **Shear behavior of polymer micro-scale truss structures formed from self-propagating polymer waveguides**, Acta Materialia, Volume 56, Issue 6, April 2008, Pages 1209-1218, ISSN 1359-6454, http://dx.doi.org/10.1016/j.actamat.2007.11.018.

been investigated experimentally, and the results indicate a strong correlation to analytical predictions based on stretch-dominated behavior [8].

Recent work has demonstrated that cellular materials with truss features on the micrometer-scale can be fabricated from an interconnected pattern of self-propagating polymer waveguides [13]. These cellular structures are highly ordered and, because of the self-propagating nature of the synthesis, they can be fabricated to be multiple unit cells thick with a single UV exposure. In addition, the process itself affords great flexibility in the resulting cellular architecture. In previous work, the compressive behavior of these micro-truss structures has been correlated to variations in density, cell size, truss angle and the properties of the solid polymer [14]. In the present work, we investigate the shear behavior of these micro-truss structures. Shear loading was applied to each sample using a single-lap shear fixture, and the measured moduli were compared with analytical predictions. In addition, the failure mechanisms for each structure were closely examined to enable an accurate prediction of the peak shear strength.

2. Microtruss architecture

The cellular architecture of the micro-truss structures investigated in this work is illustrated in Fig. 1a. Fig. 1b shows a single unit cell that defines the truss angle (θ), truss member length (l) and outer unit cell dimensions (L, H). The polymer microtruss structures were formed from an interpenetrating pattern of self-propagating polymer waveguides. The details of the synthesis technique used to create the cellular architecture shown are described elsewhere [13] and [14].

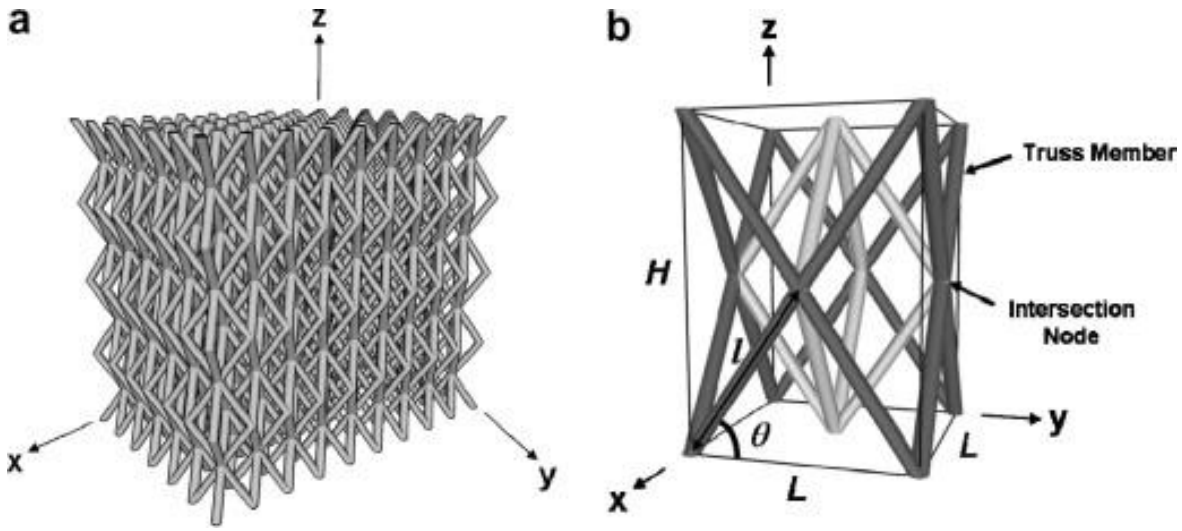

Fig. 1. *(a) Illustration of a micro-truss structure and (b) the octahedral unit cell. The darker truss members in (b) are shared with the respective adjacent unit cell [14].*

A top view of the repeating unit cell is shown in Fig. 2. The shear force (V) is defined in the x–y plane and the direction of the shear force is identified by the angle ψ. Based on the symmetry of the octahedral unit cell, the shear response will be periodic in $\psi = \pi/2$.

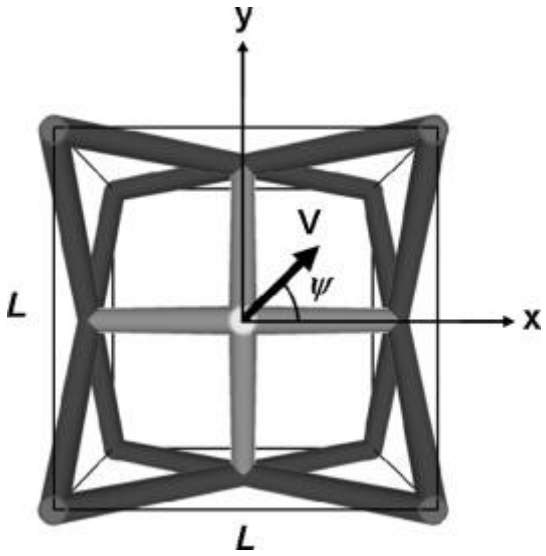

Fig. 2. *Top view of the unit cell defining the shear force direction ψ in the x–y plane.*

Please cite this article as: Alan J. Jacobsen, William Barvosa-Carter, Steven Nutt, **Shear behavior of polymer micro-scale truss structures formed from self-propagating polymer waveguides**, Acta Materialia, Volume 56, Issue 6, April 2008, Pages 1209-1218, ISSN 1359-6454, http://dx.doi.org/10.1016/j.actamat.2007.11.018.

3. Analytical predictions for shear modulus and shear strength

By symmetry of the microstructure, a force–displacement analysis can be conducted on a 1/4 unit cell, as shown schematically in Fig. 3. A shear force V that generates a displacement Δ at node A (in the direction $\psi = 0°$) will create a tensile reactive force (F_t) in truss member AB and a compressive reactive force (F_c) in truss member AD. Truss members AC and AE will exhibit a reactive moment (M) under this loading condition if nodes C and E are considered fixed. To predict the effective shear modulus (G) of the structure, the following expression was derived, assuming the external work ($V\Delta$) on the structure was equal to the work required to axially deform truss members AB and AD and to bend truss members AC and AE:

$$G = \frac{E}{8}\left(\frac{\rho}{\rho_s}\right)\left[\sin^2 2\theta + \left(\frac{9}{2}\right)\left(\frac{r\sin\theta}{l}\right)^2\right] \tag{1}$$

where (ρ/ρ_s) is the relative density of the structure defined by

$$\frac{\rho}{\rho_s} = \frac{2\pi r^2}{l^2\cos^2\theta\ \sin\theta} \tag{2}$$

The term $(r \sin\theta/l)^2$ in Eq. (1) is the contribution to G from the reactive moments generated from truss members AC and AE. For the unit cell geometries under consideration here, this contribution is negligible. If a similar analysis is conducted for a shear force in the direction $\psi = 45°$ and only axial deformation of the truss members is considered, an equivalent expression for the effective shear modulus can be derived. This indicates that because of the symmetry of the microstructure, the elastic response due to a shear load applied in the x–y plane is effectively independent of ψ [8].

Please cite this article as: Alan J. Jacobsen, William Barvosa-Carter, Steven Nutt, **Shear behavior of polymer micro-scale truss structures formed from self-propagating polymer waveguides**, Acta Materialia, Volume 56, Issue 6, April 2008, Pages 1209-1218, ISSN 1359-6454, http://dx.doi.org/10.1016/j.actamat.2007.11.018.

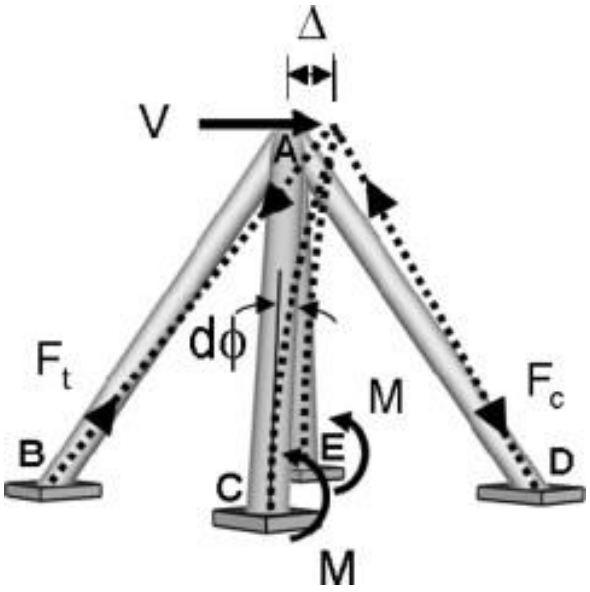

Fig. 3. *A schematic of a partial unit cell displaced Δ at node A from the shear force V.*

While the effective shear modulus is independent of the shear force direction, the shear strength of the octahedral microstructure depends on ψ. Assuming pinned nodes, the shear strength (τ_p) is given by

$$\tau_p = \frac{\sigma_p}{4}\frac{\sin 2\theta}{\cos\psi}\left(\frac{\rho}{\rho_s}\right) \tag{3}$$

where $|\psi| \leqslant \pi/4$, and, by symmetry of the unit cell, τ_p is periodic in ψ [8]. Based on this analysis, the minimum shear strength of the microstructure should occur when the shear load direction $\psi = 0°$ and the maximum should occur when $\psi = 45°$. Also, the peak shear strength is directly proportional to the peak axial failure stress in the truss members (σ_p), which is dependent on the initial failure mode of the truss members. Competing mechanisms that will ultimately determine σ_p include buckling of the truss members and tensile yielding or fracture of the polymer.

Please cite this article as: Alan J. Jacobsen, William Barvosa-Carter, Steven Nutt, **Shear behavior of polymer micro-scale truss structures formed from self-propagating polymer waveguides**, Acta Materialia, Volume 56, Issue 6, April 2008, Pages 1209-1218, ISSN 1359-6454, http://dx.doi.org/10.1016/j.actamat.2007.11.018.

4. Experimental

4.1 Parent material properties

The photomonomer used for polymer micro-truss fabrication was a thio-lene monomer system, which included 0.05 wt.% 2,2-dimethoxy-2-phenylacetophenone (Aldrich) as the photoinitiator [13]. As described in the previous section, the shear response of micro-truss structures with octahedral unit cells will depend on the tensile and compressive behavior of the solid polymer. Previously, we examined the compressive behavior of this photopolymer [14]. However, because the modulus and strength of a polymer can vary greatly for tension and compression [15], we conducted tensile tests following standard methods [16] to characterize the solid polymer.

Different post-curing treatments were used for the micro-truss samples subjected to shear testing, so multiple tensile samples of the photopolymer were fabricated under these different conditions. Four solid polymer tensile samples were first cured under collimated UV light generated from a mercury arc lamp. An exposure time of 30 s at a fluence of approximately 7.5 mW cm^{-2} was used and measured from a UV photometer sensitive to wavelengths between 300 and 400 nm (International Light Inc.). Two of the samples were then post-cured at 130 °C for 24 h under vacuum, while two other samples were post-cured at 250 °C in air. The higher-temperature post-cure in air was intended to oxidize the polymer and thus increase the modulus [17] and [18]. In Fig. 4, the tensile stress–strain curves for these samples are compared with compression data [14]obtained from the polymer processed under the same conditions.

Please cite this article as: Alan J. Jacobsen, William Barvosa-Carter, Steven Nutt, **Shear behavior of polymer micro-scale truss structures formed from self-propagating polymer waveguides**, Acta Materialia, Volume 56, Issue 6, April 2008, Pages 1209-1218, ISSN 1359-6454, http://dx.doi.org/10.1016/j.actamat.2007.11.018.

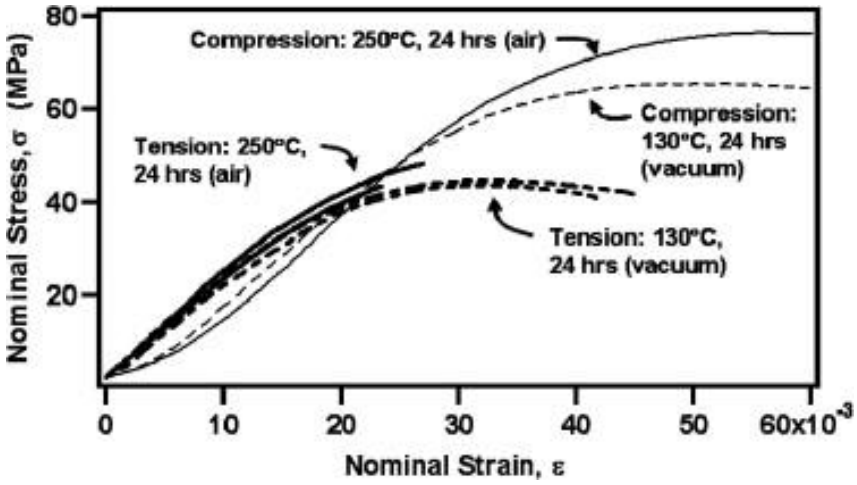

Fig. 4*. Comparison of the tensile and compressive [14] response of the solid photopolymer with different post-cure conditions.*

The tensile moduli for the four samples were determined from the initial slope of their respective stress–strain curves and the accuracy of all reported shear stress data is ±2%. The average tensile modulus ($E_{s,t}$) of the samples post-cured at 130 was 2.2 GPa, whereas the average measured compressive modulus was $E_{s,c}$ = 2.4 GPa [14]. Therefore, an average value of E = 2.3 GPa was used in Eq. (3) to predict the shear modulus. As with the compression samples, the tensile modulus of the bulk polymer post-cured at 250 °C in air ($E_{s,t}$ = 2.3 GPa) was slightly greater than the samples post-cured at 130 °C. This slight increase in the modulus measured from the samples post-cured is an oxidizing environment is attributed to an increase in cross-link density and the thin surface oxidation layer (~50 μm). Because the surface oxidation layer is only a small fraction of the overall volume of the solid polymer, the tensile modulus measured from these samples does not adequately represent the modulus of this oxidized region. We estimate that the tensile modulus of the oxidized polymer should be 3.2 GPa, based on the compression experiments on oxidized micro-truss samples [14].

Please cite this article as: Alan J. Jacobsen, William Barvosa-Carter, Steven Nutt, **Shear behavior of polymer micro-scale truss structures formed from self-propagating polymer waveguides**, Acta Materialia, Volume 56, Issue 6, April 2008, Pages 1209-1218, ISSN 1359-6454, http://dx.doi.org/10.1016/j.actamat.2007.11.018.

The tensile yield strength of the polymer was 30–40% less than the respective compressive yield strength, a finding that is consistent with observations for similar polymers [15]. The tensile samples post-cured at 130 °C under vacuum deformed plastically prior to fracture. The onset of plastic deformation in the samples post-cured at 250 °C in air was delayed, and the fracture in these samples occurred at a much lower strain. Both the increased cross-link density and an oxidized surface are known to decrease the fracture toughness of a polymer, promoting brittle failure [18].

The density of the non-oxidized polymer was measured using a gas pycnometer, yielding a value of $\rho_s = 1.34 \pm 0.01$ g cm^{-3}. The density of the oxidized region of the polymer was measured from a micro-truss sample that had been post-cured at 250 °C in air. The high surface area per unit volume and the small length scale of the micro-truss features resulted in nearly complete oxidation of the polymer during the post-cure cycle. Thus the density measurement from the solid polymer comprising the microtruss sample post-cured at 250 °C, which yielded 1.42 ± 0.01 g cm^{-3}, was taken as the density of the oxidized polymer [14].

4.2 Micro-truss samples for shear loading

A total of nine micro-truss samples were fabricated for shear testing. All samples were produced in the fabrication set-up discussed previously using an identical mask [13] and [14]. The mask consisted of a square pattern of circular apertures spaced 900 μm apart, each with a radius of 50 μm. The thickness of each micro-truss structure was approximately 5 mm (3 unit cells), which was ultimately determined from the depth of the mold containing the monomer. All samples were cut to approximately 20 mm × 20 mm square with a razor blade, and the sample dimensions were measured

using a digital caliper with 0.01 mm precision. The tolerance of each measured dimension was ±0.1 mm.

After micro-truss fabrication, the structure remained attached to the quartz plate that separated the mask and monomer. An additional quartz plate was fixed to the opposite free surface with a thin layer (~50 μm) of the same photopolymer. The samples were then post-cured for 24 h at either 130 °C under vacuum or 250 °C in air, as indicated in Table 1. After post-cure, the quartz plates were cut to the size of the sample with a diamond wafering saw.

Table 1. *Summary of the density, truss angle and post-cure temperature of the micro-truss samples fabricated for shear testing*

Sample	Density, ρ(g)	Measured truss angle, θ(deg)	Calculated truss angle, θ(deg)	Post-cure temp*(°C)
1	0.165	60 ± 2	59 ± 1.2	130
2	0.198	60 ± 2	59 ± 1.2	130
3	0.207	60 ± 2	59 ± 1.2	130
4	0.168	50 ± 2	51 ± 0.8	130
5	0.201	50 ± 2	51 ± 0.8	130
6	0.217	50 ± 2	51 ± 0.8	130
7	0.207	60 ± 2	59 ± 1.2	130
8	0.206	60 ± 2	59 ± 1.2	250
9	0.199	60 ± 2	59 ± 1.2	250

*Samples post-cured at 130 °C were under vacuum.

*Samples post-cured at 250 °C were in air.

The micro-truss structures were fabricated with a truss angle $\theta \cong 50°$ or $\theta \cong 60°$. Because it was difficult to measure the exact angle from the micrographs, the reported truss angles in Table 1 were calculated from $\theta = \tan^{-1}(H/L)$, where H and L represent the average unit cell dimensions measured from the micrographs. The densities provided in Table 1 were calculated from the measured outer volume and mass of each respective structure and the known density of the solid polymer. Although

theoretically the density of each structure should be equal, the process itself led to variations in density of up to 30% [14].

4.3 Shear experiments

A single-lap shear fixture was used to test the polymer micro-truss samples under quasi-static shear loading conditions. The samples were bonded to steel shear plates with an acrylic adhesive (3 M Scotch-Weld DP810NS) and the shear plates were attached to a hydraulic load frame as shown in Fig. 5. This configuration provided a load line approximately through the diagonal of the samples. The cross-head displacement rate was 0.5 mm min^{-1} and the load was measured with a 15 kN built-in load cell. The relative displacement of the two shear plates was measured at the sample with a laser extensometer.

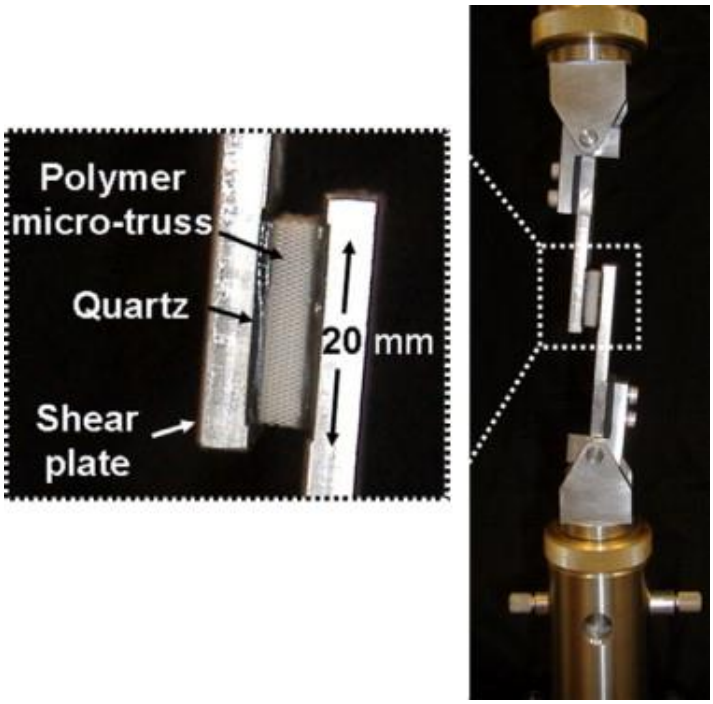

Fig. 5. *Single-lap shear fixture used to test the micro-truss samples.*

5. Results and discussion

The shear stress τ in the micro-truss samples was calculated as the measured shear load V divided by the area of the sample attached to the shear plates (A). The average shear strain λ was equal to Δ/t, where Δ is the relative displacement measured between the two shear plates and t was the thickness of the micro-truss structure [19].

The nominal shear stress–strain curves for all samples described in Table 1 are shown in Figs. 6a–c. Samples 1–6 and 8 were tested with a shear load direction $\psi = 0°$. Samples 7 and 9 were tested with a shear load direction $\psi = 45°$. Figs. 6a and 6b compare the shear response of micro-truss samples of different density but equal truss member angle, shear loading direction and post-cure cycle. Fig. 6c is a comparison of the oxidized (250 °C post-cure in air) and non-oxidized (130 °C post-cure under vacuum) samples with different shear load directions. The noticeable difference in the ultimate shear strain for Samples 1–7 is related to the distribution of deformation through the thickness of each structure during shear loading. The two oxidized samples (Samples 8 and 9) fractured prior to any significant plastic deformation.

Please cite this article as: Alan J. Jacobsen, William Barvosa-Carter, Steven Nutt, **Shear behavior of polymer micro-scale truss structures formed from self-propagating polymer waveguides**, Acta Materialia, Volume 56, Issue 6, April 2008, Pages 1209-1218, ISSN 1359-6454, http://dx.doi.org/10.1016/j.actamat.2007.11.018.

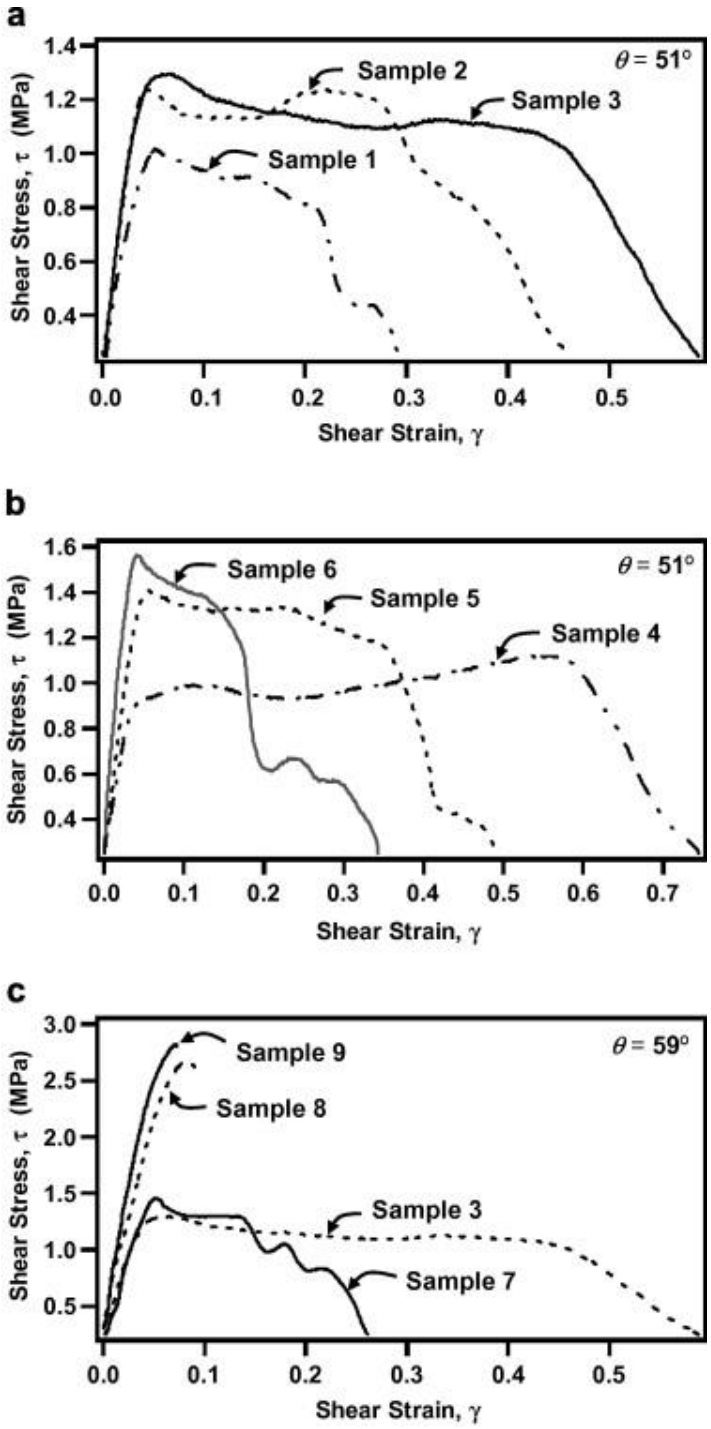

Fig. 6. *The nominal shear stress–strain curves for samples (a) post-cured at 130 °C (vacuum) with θ = 59° and a shear load direction ψ = 0°; (b) post-cured at 130 °C (vacuum) with θ = 51° and a shear load directionψ = 0°; and (c) with θ = 59° but different post-cure temperature and/or shear load direction. The accuracy of all reported shear stress data is ±2%.*

Please cite this article as: Alan J. Jacobsen, William Barvosa-Carter, Steven Nutt, **Shear behavior of polymer micro-scale truss structures formed from self-propagating polymer waveguides**, Acta Materialia, Volume 56, Issue 6, April 2008, Pages 1209-1218, ISSN 1359-6454, http://dx.doi.org/10.1016/j.actamat.2007.11.018.

5.1 Shear modulus

The shear modulus G for each sample was determined from the average slope of the respective nominal shear stress–strain curve. Linear regression was used to determine the slope between 25% and 75% of the respective peak shear stress values. At a stress below 25% of the maximum for each sample, effects from the fixture on the measured load were apparent. At a stress level above 75% of the maximum, the shear stress–strain response for most samples began to deviate noticeably from linear behavior. The measured shear moduli, along with the predicted shear moduli values calculated from Eq. (1), are shown in Table 2.

Table 2. *Summary of the shear properties for the different micro-truss samples*

Sample	Relative density ρ/ρ_s	Calculated truss angle, θ(deg)	Shear force direction, ψ (deg)	Shear modulus, G (MPa)			Measured shear strength, τ_p (MPa)	Calculated truss member stress, σ_p(MPa)
				Prediction	Measured	% error		
1	12.3	59 ± 1.2	0	28	22 ± 0.3	+28	1.0	37
2	14.8	59 ± 1.2	0	33	29 ± 0.1	+14	1.2	38
3	15.4	59 ± 1.2	0	35	31 ± 0.2	+10	1.3	38
4	12.5	51 ± 0.8	0	34	19 ± 0.1	+81	0.9	30
5	15.0	51 ± 0.8	0	41	29 ± 0.2	+43	1.4	38
6	16.2	51 ± 0.8	0	45	40 ± 0.3	+11	1.6	35
7	15.4	59 ± 1.2	45	35	34 ± 0.3	+1	1.5	30
8	14.5	59 ± 1.2	0	45	35 ± 0.1	+29	2.7	83
9	14.0	59 ± 1.2	45	44	47 ± 0.2	−6	2.8	65

Please cite this article as: Alan J. Jacobsen, William Barvosa-Carter, Steven Nutt, **Shear behavior of polymer micro-scale truss structures formed from self-propagating polymer waveguides**, Acta Materialia, Volume 56, Issue 6, April 2008, Pages 1209-1218, ISSN 1359-6454, http://dx.doi.org/10.1016/j.actamat.2007.11.018.

Samples 1–3, which had the same truss member angle θ and were tested under the same shear load direction ψ, showed an increase in the deviation between the predicted and measured shear modulus with a decrease in relative density. Samples 4–6 exhibited a similar trend. These data indicate that as the relative density of micro-truss structures with equal unit-cell geometry decreases, the structures become more susceptible to non-ideal deformation, such as truss member bending and twisting.

The data in Table 2 also imply that for micro-truss structures of approximately equal relative density, there is a greater deviation between the measured and predicted modulus when the truss member angle θ is reduced (Samples 4–6). For a fixed micro-truss thickness, the polymer waveguides that form the truss members have to propagate farther if there is a reduction in truss member angle [13]. Although theoretically, the shear modulus should increase as θ approaches 45°, the necessary increase in waveguide propagation distance leads to a greater likelihood of initial structural defects, such as truss member curvature and/or misalignment. This causes a greater reduction in the measured modulus values, as reflected in the data.

Sample 8 was post-cured in an oxidizing environment (250 °C in air for 24 h), and had approximately the same relative density and truss member angle as Sample 2. Thermo-oxidation of the polymer leads to an increase in solid polymer modulus [14], which is directly proportional to the shear modulus of these structures, as shown in Eq. (1). As with Samples 1–6, the difference between predicted and measured modulus values was attributed to non-ideal deformation, such as bending of the truss members, prior to reaching the peak strength.

Please cite this article as: Alan J. Jacobsen, William Barvosa-Carter, Steven Nutt, **Shear behavior of polymer micro-scale truss structures formed from self-propagating polymer waveguides**, Acta Materialia, Volume 56, Issue 6, April 2008, Pages 1209-1218, ISSN 1359-6454, http://dx.doi.org/10.1016/j.actamat.2007.11.018.

Two samples were tested with a shear force direction ψ = 45° (Samples 7 and 9). The measured modulus values for both samples were much closer to the predicted values than Samples 1–6 and 8. While the shear modulus in principle should be independent ofψ, these observations can be understood in terms of the load distribution between the truss members for the different shear load directions. When the shear force is applied in the direction ψ = 0°, nearly all the load is carried by only half of the truss members (those parallel to the shear load, at ψ = 0°). The truss members perpendicular to the shear load (at ψ = ±90°) contribute little to the shear resistance, as determined from Eq. (1). If the shear force is applied in the direction corresponding to ψ = 45°, the load is distributed approximately equally between all truss members (half are in tension and half are in compression). Thus, for a given applied shear load, the actual maximum stress in the truss members is greater when ψ = 0° than when ψ = 45°. Under ideal linear elastic conditions, this difference in load distribution would only affect the shear strength of the micro-truss. However, we conclude that for the polymer micro-trusses, a more uniform distribution of load between the truss members reduces the degree of non-ideal deformation in the truss members, thus increasing the measured modulus.

5.2 Shear experiments

The shear strength of the polymer micro-truss structures depends on the initial failure mode of the truss members. As shown in Fig. 3, the tensile yield strength of the solid polymer is significantly less than the compressive yield strength, and thus initial failure is expected in those truss members under tension. However, in studies on the compression behavior of these structures, buckling of the truss members occurred at a stress level well below predicted values [14]. These competing

mechanisms – compression buckling and tensile failure of the truss members – will ultimately determine how the structures fail.

Table 2 shows the measured shear strength τ_p for each sample, as well as the estimated peak stress in the truss members at initial shear failure. The average peak stress in the truss members was calculated by solving for σ_p in Eq. (3). Samples 1–6, with a shear load direction $\psi = 0°$, had an estimated average truss member stress between 30 and 40 MPa at initial failure, which is approaching the tensile strength of the polymer. This indicates that shear failure was likely to initiate from the onset of tensile yielding, which subsequently caused the compressive members to carry additional load and ultimately buckle.

After reaching the peak shear strength, continued loading produced a stress plateau, followed ultimately by truss rupture. The net strain over which the stress plateau occurred was markedly different between samples. Micrographs of the structures after complete shear failure showed the total plateau strain was dependent on how uniformly the deformation was distributed through the thickness of the structure. For example, Fig. 7a shows Sample 4, which had the greatest plateau strain, after shear testing. The micrograph shows that truss members under compression buckled uniformly through the thickness of the structure. In contrast, Sample 2 produced roughly half the total plateau strain compared with Sample 4, and the failure was localized in a single cell layer, as shown in Fig. 7b. Fig. 7c is a close-up of a fracture surface of Sample 2 in which the crack did not propagate through the entire truss member.

Please cite this article as: Alan J. Jacobsen, William Barvosa-Carter, Steven Nutt, **Shear behavior of polymer micro-scale truss structures formed from self-propagating polymer waveguides**, Acta Materialia, Volume 56, Issue 6, April 2008, Pages 1209-1218, ISSN 1359-6454, http://dx.doi.org/10.1016/j.actamat.2007.11.018.

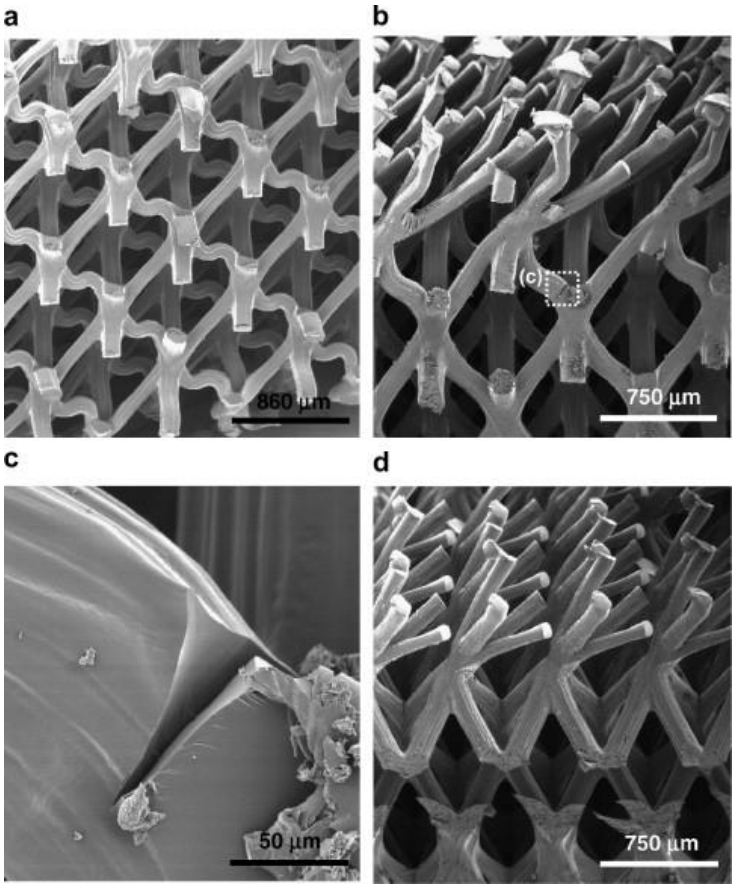

Fig. 7. *SEM images displaying different shear failure modes in the micro-truss structures. (a) Sample 4, (b) Sample 2, (c) close-up of a crack on a buckled truss member in Sample 2, and (d) Sample 7.*

As shown in Eq. (3), the shear strength for a micro-truss sample with a shear load direction $\psi = 45°$ should be greater (by 41%) than an equivalent sample with a shear load direction $\psi = 0°$. Samples 3 and 7 have equivalent unit cell structures and relative density, yet the shear strength of Sample 7 (with $\psi = 45°$) is only 15% greater than that of Sample 3 (with $\psi = 0°$). Examination of Sample 7 after shear testing (Fig. 7d) reveals that failure occurred by polymer yielding at the nodes along a single unit cell layer. The different mode of failure for this structure accounts for the discrepancy between measured and predicted strength values.

The two oxidized samples (8 and 9) showed a significant increase in shear strength compared with the other samples, and this was consistent with expectations based on previous compression

experiments [14]. Again, the analytical expressions predicted different shear strengths for these two samples based on different shear load directions. However, as with Samples 3 and 7, the shear strengths were approximately equal. Also, as shown in Fig. 6c, the brittle nature of these samples led to abrupt failure at the peak load without the subsequent stress plateau that was characteristic of the unoxidized samples.

Inspection of the fracture surfaces of Samples 8 and 9 provides insight into the process by which these structures failed. Fractography defines three distinct regions associated with the dynamics of a fracture surface: mirror, mist and hackle [20]. The mirror region is the smooth surface that forms during initial slow crack growth in a material. As the stress in the material increases and the critical stress intensity factor (K_{Ic}) is reached, the crack becomes unstable and rapid crack growth ensues. This causes the hackle region of a fracture surface. The mist region is the transition between mirror and hackle, and is often difficult to clearly identify [20].

Fig. 8 a is a micrograph of a fractured region in Sample 8, and Fig. 8b–d are close-up images of the fracture surfaces for adjacent individual truss members. The direction of the shear load V ($\psi = 0°$) indicates that the fracture surface shown in Fig. 8b corresponds to a truss member under compression. Based on comparisons with fractography of optical fibers [21], we concluded that the fracture surface shown in Fig. 8b was caused by slight bending of the truss member under compression. The mirror regions in Figs. 8c–e represent the degree of crack propagation prior to failure. As cracks formed under tension and bending/twisting in these truss members, the load carried in the compression member increased. Upon failure of the compression truss members, the sudden increase in load on the remaining truss members led to rapid failure, causing the distinct hackle regions in Figs. 8c–e.

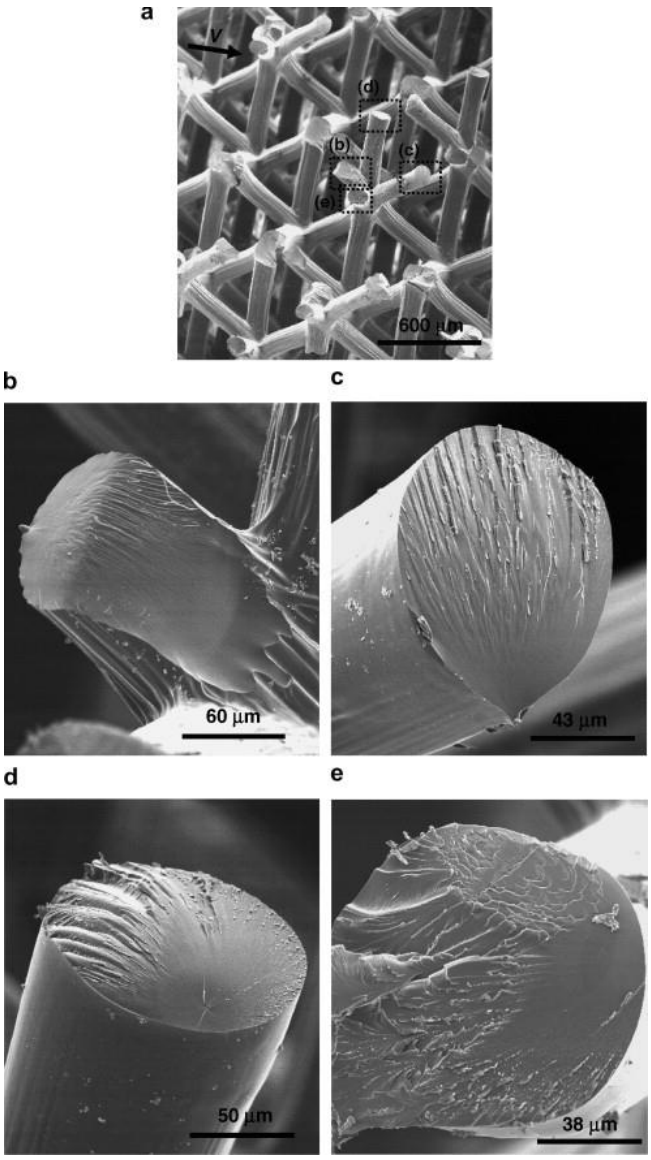

Fig. 8*. Truss member fracture surfaces of Sample 8 which had a shear force direction* $\psi = 0°$.

The fracture surfaces of a single unit cell in the thermally oxidized Sample 9 are shown in Fig. 9a. Figs. 9b–e are enlargements of the individual fractured truss members. The location of the mirror and hackle regions in these truss members with respect to the shear load direction indicates that bending and twisting of all truss members occurred prior to failure. In addition, the similarity in all four fracture surfaces suggests a more uniform distribution of load between the truss members in comparison with Sample 8. Theory predicts that failure in Sample 9 should occur at a greater stress

Please cite this article as: Alan J. Jacobsen, William Barvosa-Carter, Steven Nutt, **Shear behavior of polymer micro-scale truss structures formed from self-propagating polymer waveguides**, Acta Materialia, Volume 56, Issue 6, April 2008, Pages 1209-1218, ISSN 1359-6454, http://dx.doi.org/10.1016/j.actamat.2007.11.018.

than Sample 8. However, the complex state of stress in each truss member generated from the constraint at the nodes was not taken into account in the analytical prediction. We believe this complex state of stress contributed to the reduced shear strength observed for the micro-truss structure.

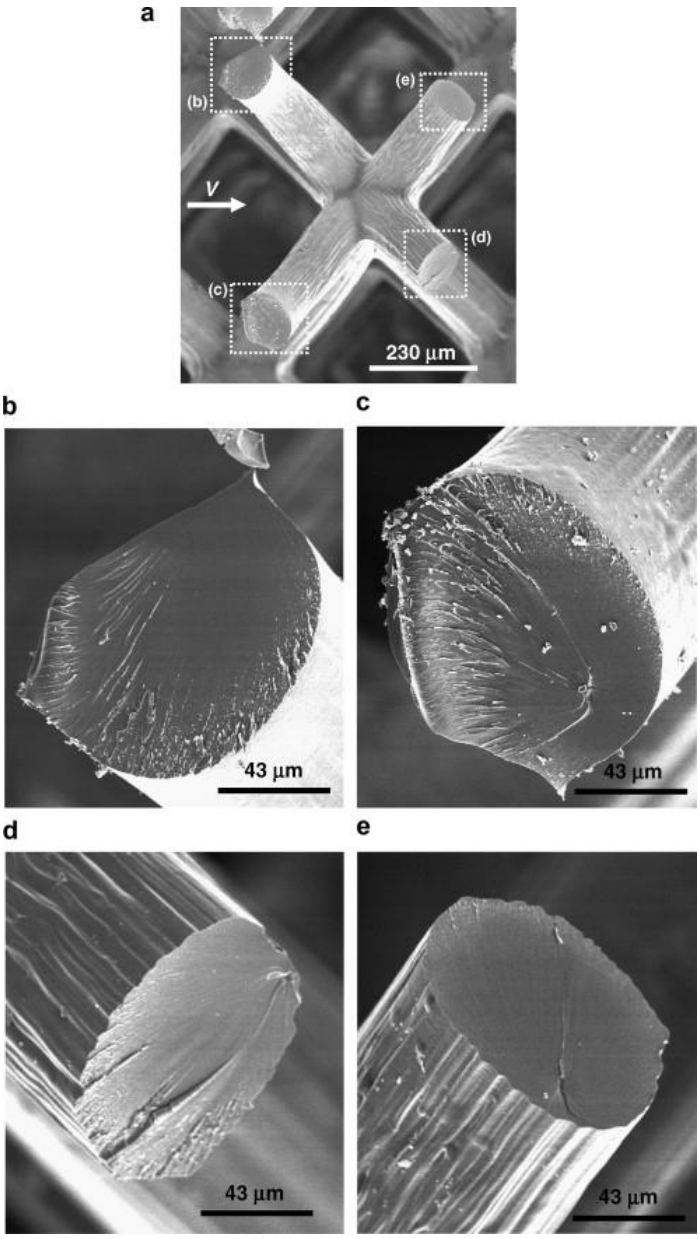

Fig. 9. *Truss member fracture surfaces of thermally oxidized Sample 9, in which the shear force direction was* $\psi = 45°$.

Please cite this article as: Alan J. Jacobsen, William Barvosa-Carter, Steven Nutt, **Shear behavior of polymer micro-scale truss structures formed from self-propagating polymer waveguides**, Acta Materialia, Volume 56, Issue 6, April 2008, Pages 1209-1218, ISSN 1359-6454, http://dx.doi.org/10.1016/j.actamat.2007.11.018.

6. Conclusions

Shear experiments were conducted on polymer micro-truss structures. The results showed that for structures of equivalent unit cell geometry, the measured shear modulus deviated from predicted values in inverse proportion to the relative density. When the shear force was applied in a direction that distributed the load uniformly between all truss members ($\psi = 45°$), the sensitivity to non-ideal deformation was reduced, and the measured shear modulus values were consistent with analytical predictions.

The shear strength of the micro-truss structures depended on the tensile and compressive strength of the polymer, as well as on the failure mode of the structure. For the unoxidized polymer micro-truss structures, tensile yielding promoted bucking of the truss members under compression. The ultimate plateau strain after initial truss member failure was determined by non-localized distribution of buckling members through the thickness of the structure. When buckling was distributed evenly through the thickness, uniform plateau shear strains of up to 60% were possible. However, when buckling was localized primarily in a single layer, this plateau strain was reduced twofold or more. Thus, to maximize energy absorption from shear failure – which is directly proportional to the area under the shear stress–strain curve – designing and fabricating a structure in which failure is uniformly distributed through the thickness is essential.

To increase the shear strength and modulus of these structures, micro-truss samples were post-cured in an oxidizing environment. The shear strength and modulus increased as expected, but the trusses were embrittled, and complete fracture occurred in the structure at the peak load. While this behavior is undesirable for energy absorption, similar post-cure cycles could be utilized to produce ultra-

Please cite this article as: Alan J. Jacobsen, William Barvosa-Carter, Steven Nutt, **Shear behavior of polymer micro-scale truss structures formed from self-propagating polymer waveguides**, Acta Materialia, Volume 56, Issue 6, April 2008, Pages 1209-1218, ISSN 1359-6454, http://dx.doi.org/10.1016/j.actamat.2007.11.018.

lightweight open-celled structures with high shear and bending strength and stiffness. Additional improvements in the overall shear properties of the polymer microtruss structures should be possible through further reductions in feature size and new processing methods that promote molecular alignment along truss members, analogous to polymer fiber processing, thereby enhancing the tensile properties of the trusses.

Acknowledgements: A.J.J. would like to thank the National Physical Science Consortium for fellowship support. Also, the authors thank Chaoyin Zhou (HRL) for his valuable assistance and Bob Doty (HRL) for the SEM micrographs and his helpful discussions on fractography.

References:

1. Gibson LJ, Ashby MF. Cellular solids: structure & properties. seconded. Cambridge: Cambridge University Press; 1997.
2. Deshpande VS, Ashby MF, Fleck NA. Acta Mater 2001;49:1035.
3. Ashby MF. Phil Trans R Soc A 2006;364:15.
4. Wadley HNG. Phil Trans R Soc A 2006;364:31.
5. Brittain ST, Sugimura Y, Schueller OJA, Evans AG, Whitesides GM. J Microelectromech Syst 2001;10:113.
6. Wadley HNG. Adv Eng Mater 2002;4:726.
7. Chiras S, Mumm DR, Evans AG, Wicks N, Hutchinson JW, Dharmasena K, et al. Int J Solids Struct 2002;39:4093.
8. Deshpande VS, Fleck NA. Int J Solids Struct 2001;38:6275.
9. Hyun S, Karlsson AM, Torquato S, Evans AG. Int J Solids Struct 2003;40:6989.
10. Wadley HNG, Fleck NA, Evans AG. Compos Sci Technol 2003;63:2331.
11. Wallach JC, Gibson LJ. Int J Solids Struct 2001;38:7181.
12. Wicks N, Hutchinson JW. Mech Mater 2004;36:739.
13. Jacobsen AJ, Barvosa-Carter W, Nutt S. Adv Mater 2007;19:3892.
14. Jacobsen AJ, Barvosa-Carter W, Nutt S. Acta Mater 2007;55:6724.
15. Nielsen LE. Mechanical properties of polymers and composites, vol.2. New York: Marcel Dekker Inc.; 1974.
16. A.S.D. 638-03, Standard Test Method for Tensile Properties of Plastics. 2003 ASTM International, West Conshohocken, PA.
17. Celina M, Graham AC, Gillen KT, Assink RA, Minier LM. Rubber Chem Technol 2000;73:678.
18. White JR. CR Chimie 2006;9:1396.
19. A.S.C. 273-00, Standard Test Method for Shear Properties of Sandwich Core Materials. 2000 ASTM International, West Conshohocken, PA.

Please cite this article as: Alan J. Jacobsen, William Barvosa-Carter, Steven Nutt, **Shear behavior of polymer micro-scale truss structures formed from self-propagating polymer waveguides**, Acta Materialia, Volume 56, Issue 6, April 2008, Pages 1209-1218, ISSN 1359-6454, http://dx.doi.org/10.1016/j.actamat.2007.11.018.

20. Hull D. Fractography: observing, measuring, and interpreting fracture surface topography. - Cambridge: Cambridge University Press; 1999.
21. Chen CP, Chang TH. Mat Chem Phys 2002;77:110.

Please cite this article as: Alan J. Jacobsen, William Barvosa-Carter, Steven Nutt, **Shear behavior of polymer micro-scale truss structures formed from self-propagating polymer waveguides**, Acta Materialia, Volume 56, Issue 6, April 2008, Pages 1209-1218, ISSN 1359-6454, http://dx.doi.org/10.1016/j.actamat.2007.11.018.